Numerical study of the influence of albedo on the microclimate of Bergpolder Zuid, Rotterdam

Yasin Toparlar*[1,2], Bert Blocken[1,3], Bino Maiheu[2], Gert-Jan van Heijst[4]

1 *Building Physics and Services, Eindhoven University of Technology, Eindhoven, the Netherlands*

2 *Environmental Modelling Unit, Flemish Institute for Technological Research, Mol, Belgium*

3 *Building Physics Section, Leuven University, Heverlee, Belgium*

4 *Fluid Dynamics Laboratory, Eindhoven University of Technology, Eindhoven, the Netherlands*

**Presenting author, e-mail: y.toparlar@tue.nl*

1. Introduction

The rapid trend towards urbanization [1] has increased the popularity of studies investigating urban microclimate. Urban Heat Islands (UHI) and summer-time heat waves can have a significant influence on human thermal comfort and building energy demand [2]. For the investigation of urban microclimate, historically, observational approaches (such as field measurements) have been employed and lately, with the advancements in computing power, computational methods are becoming more popular because of the possibility to conduct scenario analyses [3]. Computational Fluid Dynamics (CFD) is one of these computational methods which has the potential to predict urban microclimate. Compared to other computational methods employed to investigate urban microclimates (i.e. Energy Balance Models), CFD has the capability to couple the flow and temperature fields at high levels of spatial details (i.e. street canyons, individual buildings) [3]. Regarding the research on urban physics and urban microclimate, the period after 1990s is denoted as the “modeling era” where realistic models have started to emerge for numerical analysis [4] and during this period, CFD has become increasingly popular in these fields [5]. CFD analysis of urban areas requires a high-resolution 3D model of the urban location, the knowledge of relevant boundary conditions and adequate computational resources [6]. An overview of the CFD studies on the analysis of urban microclimates is provided by Toparlar et al. [7].

The focus of the paper by Toparlar et al. [7] was the validation of the surface temperatures occurring in the Bergpolder Zuid region in Rotterdam during the 2006 heat wave. The study concluded that the CFD approach followed had the potential to accurately predict urban microclimate. Another conclusion from the paper was that the same CFD approach can be used for the analysis of climate change adaptation measures (i.e. urban greening, low albedo surfaces, different material usage). Based on these conclusions, this paper focusses on the influence of surface albedo on the microclimate of Bergpolder Zuid, Rotterdam.

Several studies investigated the effect of surface albedo on urban microclimate using observational approaches [8–11] or computational methods [12–14]. For example, Rosenfeld et al. [8] investigated the effect of surface albedo on energy savings and on air temperature. In their measurement campaign conducted at New Mexico, two nearby locations with albedo values 0.6 and 0.25 were chosen for recording the air temperature data. According to their findings, air temperatures at the location with higher albedo, on average, was 3°C cooler in the morning hours and stayed cooler throughout the day. Chudnovsky et al. [9] investigated the surface temperatures in Tel-Aviv using a thermal video radiometer placed on a high-rise building. The comparison was made for pavements with different materials. In the study, the albedo values were not mentioned, but the materials were specified as dark colored asphalt, dark colored concrete, light colored concrete and granulite. According to their findings, the surface temperature on the dark colored asphalt was approximately 4-5°C higher than light colored concrete at noon. The temperature differences between these two materials at 10:00 and at 17:00 were approximately 1.0-1.5°C (warmer asphalt). The study by Doulos et al. [10] focused on 93 pavement samples with different materials and surface colors. The measurement data were collected both for air and surface temperatures. It was demonstrated that for the white versus black colored concrete pavement tiles, the mean surface temperature throughout the day differs by almost 11°C. Prado and Ferreira [11] focused on the measurement of albedo on roof materials and estimated the maximum surface temperatures based on the calculation method by Bretz et al. [15]. According to the results, a cement roof with an albedo of 0.15 was found to be approximately 8.3°C warmer than a cement roof with an albedo of 0.5.

Apart from the listed observational approaches, computational methods were also employed for the investigation of the effect of albedo on urban microclimate. One of the earliest numerical studies on this topic was conducted by Sailor [12]; in this study he numerically increased the average albedo in downtown Los Angeles by 0.14, which resulted in a potential cooling of the air temperature by 0.5°C minimum and 1.4°C maximum. Hamdi and Schayes [14] used an urban surface exchange parameterization considering a summer period in the city of Basel, Switzerland. They increased the albedo values in a street canyon by 0.16 for buildings walls and roofs, and by 0.22 for the roads. Compared with the initial case, they reported a maximum 0.6°C cooling of air temperatures and the cooling effect was reported to be noticeable throughout the entire day. In the study by Priyadarsini et al. [13] CFD simulations were performed. They used façade and roof materials in a street canyon with different albedo values of 0.04, 0.47 and 0.83. Simulation results were reported for the air temperatures inside the street canyon. Compared with the case with the highest albedo, the air temperatures were found to be 1.3°C (for albedo=0.47) and 2.5°C (for albedo=0.04) higher.

It should be noted, however, that CFD has not yet been employed extensively for the analysis of the effect of albedo on the urban climate at neighborhood scale. Studies are limited either to individual buildings/street canyon surfaces or to a complete city using a bulk-approach at lower spatial resolution. In this study, CFD simulations are performed to predict urban temperatures in the Bergpolder Zuid region, located in Rotterdam. In the first part, the surface temperatures inside the region are validated using satellite imagery data, recorded during the heat wave of July 2006 [16]. In the second part, the investigation focuses on the effect of changing surface albedo on the surface temperatures, considering the first two days of the validated time range. After the presentation of the results, the paper concludes with a discussion and a conclusions section.

2. Case description

The basic symptoms of the UHI effect in Rotterdam due to its dense urban morphology were demonstrated in several studies [16,17]. According to the satellite imagery data reported by Klok et al. [16], the average surface temperatures inside Rotterdam can reach up to 45°C during heat waves. The main area of interest in this study is the Bergpolder Zuid region, which is located in the Noord district of the city. The region is composed of both residential and office buildings. Inside the region, most of the streets can be considered as narrow with the aspect ratios ranging from 1:1 to 2:1. The dominant color on the building facades is red (bricks) and the rooftops are mainly red colored roof tiles or grey colored concrete. The average height of the buildings is 12.6 m with the lowest building having a height of 2.8 m and the highest building is 51.0 m.

3. CFD simulations: Computational settings and parameters

3.1 Computational domain and grid

For the CFD simulations of the case, the geometric shape of Bergpolder region is modelled inside a circular subdomain. Geographically, to the south of this circular subdomain, Rotterdam city center is located and to the North, mainly green fields can be found. The regions around the circular subdomain are not explicitly modelled in the CFD simulations (Figure 1a) but rather represented with an aerodynamic roughness length (z_0) based on the updated Davenport roughness classification [18] (more information on this estimation can be found in Ref. [7]).

The computational domain is composed of the circular subdomain where the urban area is modelled (Figure 1b) and a hexagonal subdomain, which is modelled for the development of airflow around the urban area. The hexagonal outer shape has an edge length of 1.2 km and a height of 400 m. The level of geometric detailing is finer in the area of interest (Bergpolder Zuid) compared with the other zones of Bergpolder. Generation of the computational grid is based on the technique as introduced by van Hooff and Blocken [19]. During the grid generation, special attention is given to the CFD best practice guidelines of Franke et al. [20] and Tominaga et al. [21]. In total, the grid consists of 6,610,456 hexahedral cells (Figure 1c).

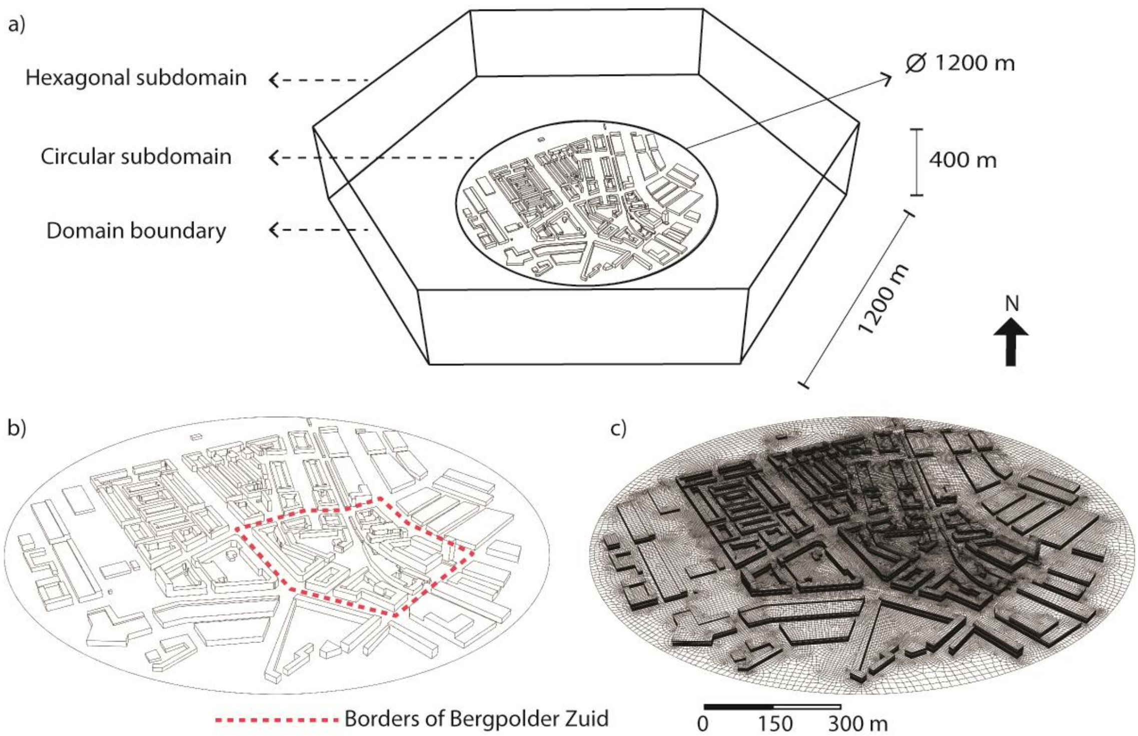

Figure 1: a) A view of the computational domain; b) Computational geometry of the circular subdomain and the borders of Bergpolder Zuid; c) Computational grid on the building and street surfaces (number of cells: 6,610,456).

3.2 Boundary conditions

In all the simulations performed, three of the boundaries on the hexagonal subdomain are defined as velocity inlets and the others as pressure outlets, meaning they have zero static pressure. The boundary types on the outer faces are specified according to the wind direction. The top of the computational domain is modeled as a slip wall, which means zero normal gradient is assumed for all the variables. Ground surface and buildings surfaces are specified as separate wall type boundaries.

At the inlets, the mean wind speed U (m/s), turbulent kinetic energy k (m^2/s^2) and turbulence dissipation rate ε (m^2/s^3) profiles are determined from the following equations [22]:

$$U(z) = \frac{u^*}{\kappa} \ln\left(\frac{z+z_0}{z_0}\right) \qquad k = \frac{u^{*2}}{\sqrt{C_\mu}} \qquad \varepsilon(z) = \frac{u^{*3}}{\kappa(z+z_0)}$$

In these equations, z_0 (m) is the aerodynamic roughness length and it is specified either as 0.5 m or as 1.0 m depending on the wind direction, κ is the von Karman constant (= 0.41), u^* (m/s) is the atmospheric boundary layer friction velocity, C_μ is the model constant (= 0.09) and z (m) is the height coordinate. At the inlets, a uniform air temperature is imposed and its value and time dependency are based on the hourly weather data acquired from the Royal Dutch Meteorological Institute (KNMI).

At the walls, the Standard Wall Functions [23] are used in combination with the sand-grain based roughness modification [24]. The appropriate relationship between k_S (roughness height) (m), C_S (roughness constant) and z_0 is satisfied with the following equation [25]:

$$k_S = \frac{9.793 z_0}{C_S}$$

As mentioned by Blocken et al. [25], in ANSYS Fluent v12.0, the k_S value cannot be specified higher than the z_P value, which is the height of the middle of the first cell close to the wall. In the computational grid generated, the first cell height is 2.8 m at the hexagonal subdomain (thus $z_{P,\,hexagonal}$ = 1.4 m) and 0.23 for the circular subdomain ($z_{P,\,circular}$ = 0.115 m). According to the equation above, for the hexagonal domain, when z_0 = 0.5 then k_S = 1.39, C_S = 3.5 and when z_0 = 1.0 then k_S = 1.39 m and C_S = 7. The ground surfaces of both hexagonal and circular subdomains are modelled implicitly as a 10 m thick earth layer with a constant temperature of 10°C at the bottom. The building walls are modelled as brick walls with 0.4 m thickness. Inside the buildings, a constant 24°C temperature is imposed to bear resemblance to air conditioned spaces during summer-time. Specifications of the materials used can be seen in Table 1. Evapotranspiration is also considered at the ground plane by implementing a constant sink value of 80 W/m^2 during morning (6:00 – 11:00) and afternoon (15:00 – 18:00) and 130 W/m^2 during noon time.

Table 1: Specifications of the materials used in this study.

Fluid	Density (kg/m^3)	Specific heat (J/kg.K)	Thermal conductivity (W/m.K)	Thermal expansion coefficient (1/K)	
Air (12.5°C)	1.242	1005	0.025	0.00342	
Solid	**Density (kg/m^3)**	**Specific heat (J/kg.K)**	**Thermal conductivity (W/m.K)**	**Absorptivity**	**Emissivity**
Earth	1150	650	1.5	0.6	0.90
Brick	1400	900	1.7	0.75	0.88

3.3 Other computational settings and parameters

The 3D Unsteady Reynolds-averaged Navier Stokes (URANS) equations are solved in combination with the realizable k-ε turbulence [26] model for closure. Radiation is handled with the P-1 radiation model [27] and the Boussinesq approximation is used for buoyancy effects. Pressure-velocity coupling is taken care of by the SIMPLE algorithm. For convection and viscous terms, second order discretization schemes are used and second order implicit time integration is imposed for temporal discretization. Unsteady simulations are performed with 15-minute time steps and each time step is calculated with 100 iterations. Simulations are performed continuously, meaning no interruption or initialization process had taken place during the simulation of consecutive days.

4. CFD simulations I: Validation of surface temperatures

In an earlier study by Klok et al. [16] averaged surface temperatures over different districts of Rotterdam were reported using satellite imagery data recorded by the Advanced Very High Resolution Radiometer (AVHRR) during 15-19 July 2006. The aim of this part of the study was to perform simulations for the same five consecutive days and to compare the resulting average surface temperatures with the satellite imagery data. Meteorological data for these dates are acquired from the KNMI Rotterdam weather station and it is provided in Figure 2. The wind direction on 15, 16, 17 and 19 July was mainly from North, Northeast and East, whereas on 18 July some southeast wind was also observed. The results for the average surface temperatures in the region is based on the average of 90 control points placed on the building and street surfaces over Bergpolder Zuid. The choice for the amount of control points is based on a sensitivity analysis which is further described in Ref. [7]. Simulations are performed for the five days in which the satellite imagery data was recorded. In total, Klok et al. [16] have reported 42 instantaneous values of average surface temperatures. Considering the fact that the KNMI meteorological data is based on hourly averaged values, it is likely that some deviation might exist between the weather conditions at the instances of satellite images and the data acquired.

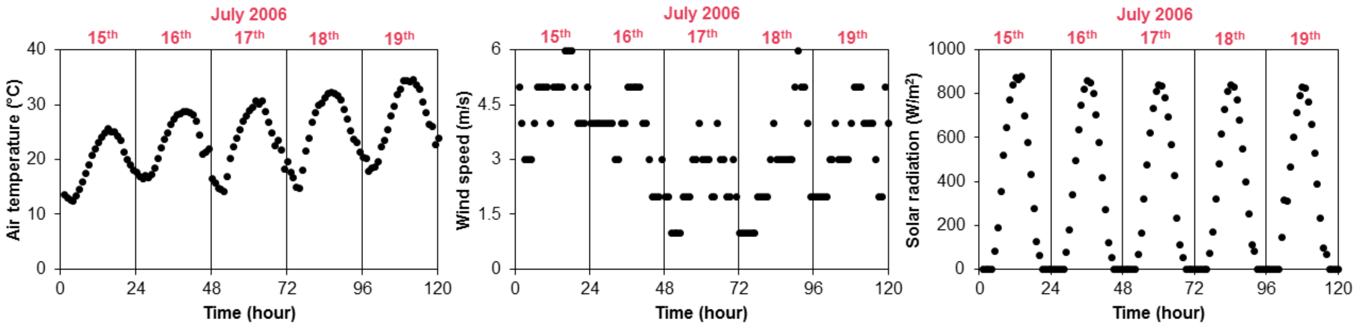

Figure 2: Meteorological data of Rotterdam (from the KNMI Rotterdam weather station) for 15-19 July 2006. The data acquired contains information for air temperature (°C), wind speed (m/s) and solar radiation (w/m²)

The resulting surface temperatures from the CFD simulations are presented in Figure 3 along with the satellite imagery data. Overall, a fairly good agreement can be observed especially in repeating the general trend of daily surface temperatures. Average difference between the CFD simulations and satellite imagery data was found to be around 7.91% whereas the minimum deviation is 0.27% and the maximum is 24.24%. An overall problem in predicting the surface temperatures for the noontime of 18 July can be observed. This might be related to the uncertainty in the satellite imagery data or to the differences in the actual solar radiation due to cloud cover over the region and the one reported by the meteorological station.

With the simulations performed, it is possible to observe the effect of heat storage mechanism on urban microclimate as the heat which is stored within the building materials is released throughout the nighttime. Moreover, simulations are also helpful for the determination of the locations with low wind velocity, which results with higher surface temperatures. As the simulations predicted the surface temperatures with reasonable accuracy, it was concluded that the CFD approach followed can be used for further studies to analyze climate change adaptation measures.

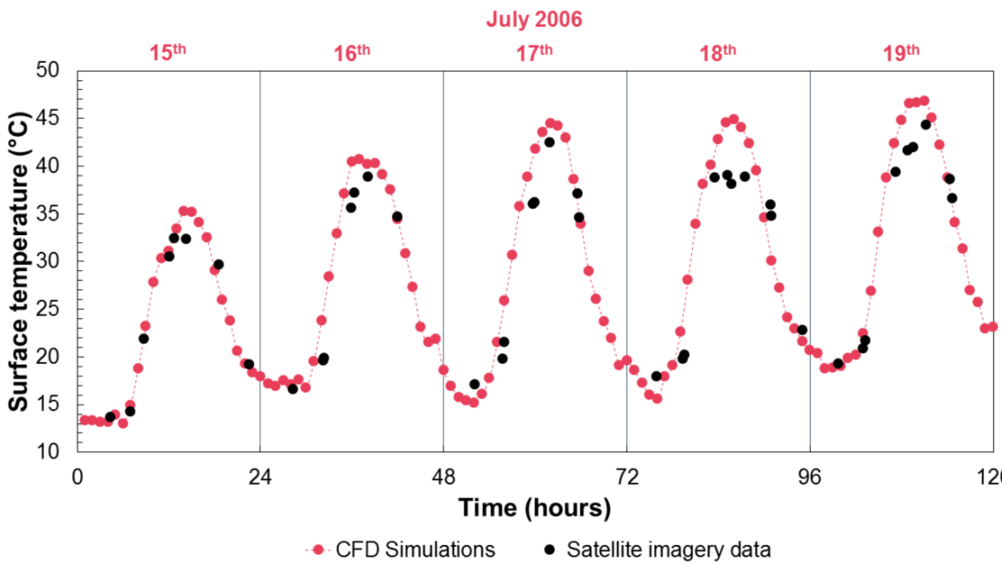

Figure 3: Comparison of simulation results and data from satellite images with respect to average surface temperatures for five consecutive days.

5. CFD simulations II: Effect of albedo on urban microclimate

One of the advantages of CFD for the analysis of urban microclimate is the possibility to consider different scenarios for the urban environment in question. In this part of the study, the investigation focused only on the first two days period from the original study. The effect of albedo is evaluated based on the following comparisons:

1) *Comparison 1:* The original study, a case with higher albedo (15% higher than original) on building surfaces (façade and roofs) and ground surfaces, a case with lower albedo (15% lower than original) on building and ground surfaces.
2) *Comparison 2:* The original study, a case with higher albedo (15% higher than original) on building and ground surfaces, a case with higher albedo (15% higher) only on building surfaces, a case with higher albedo (15% higher) only on ground surfaces.

The comparisons focused on the average surface temperatures, using the same methodology of control points as described in the previous section. The results of *comparison 1* is provided in Figure 4 and the results of *comparison 2* is provided in Figure 5.

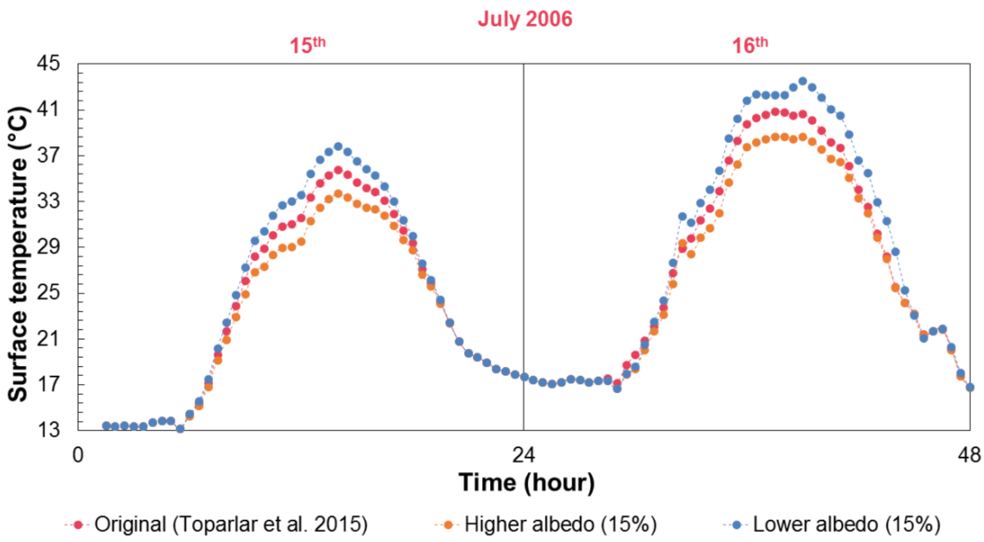

Figure 4: Comparison of average surface temperatures based on the CFD simulations for: original study, case with higher albedo and case with lower albedo.

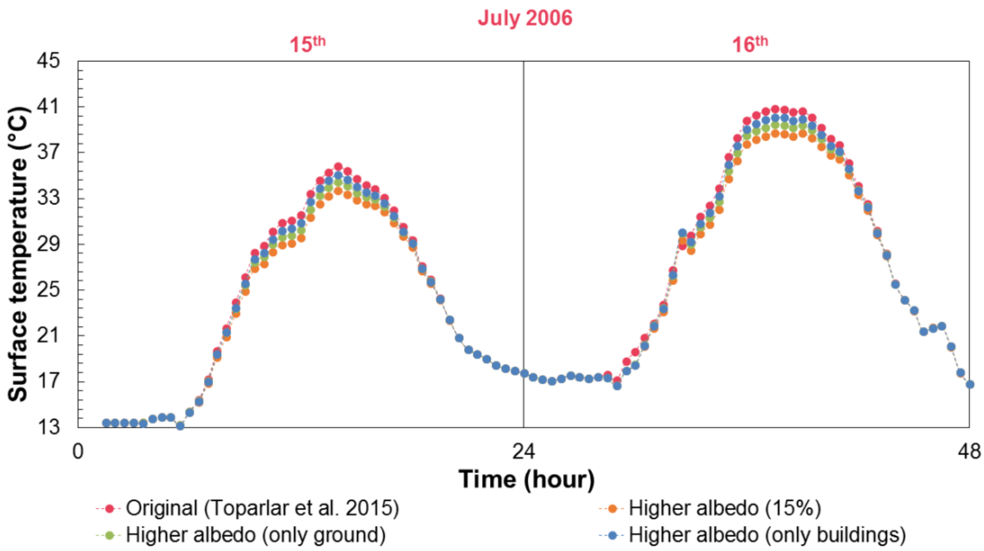

Figure 5: Comparison of average surface temperatures based on the CFD simulations for: original study, case with higher albedo, case with higher albedo only imposed on ground level and case with higher albedo imposed only on buildings.

According to the results of the *comparison 1*, increasing the albedo by 15% can lower the average surface temperatures by 2.18°C (maximum), 0.79°C (24h average) and 1.54°C (12h average). On the other hand, decreasing the albedo of the building and ground surfaces by 15% can cause an increase on the average surface temperatures by 3.13°C (maximum), 0.96°C (24h average) and 1.72°C (12h average). The 12h average considers the time from 6:00 in the morning till 18:00 in the evening, where the solar radiation is more effective.

As for the *comparison 2*, increasing only the albedo of building surfaces can decrease the average surface temperatures by 1.19°C (maximum), 0.32°C (24h average) and 0.56°C (12h average). Increasing the albedo of ground surfaces only can decrease the average surface temperatures by 1.41°C (maximum), 0.48°C (24h average) and 0.94°C (12h average). It may be noticed from Figure 5 that changing the albedo on the ground surfaces is more effective in decreasing the average surface temperatures than changing the albedo of building surfaces. This is mostly because the average temperatures on ground surfaces are in general higher than the temperatures of building surfaces and therefore a decrease of albedo with the same percentage is more effective on the ground. In addition, among the 90 sampling points, the ratio between the points located on the streets and on the rooftops can have an influence on the resulting average surface temperatures.

6. Discussion

Considering the validation study, the deviation of the results from the measurements can be due to several reasons: 1) The one-directional wall conduction approach might not be sufficient to repeat the complexity of heat transfer at the ground; 2) The effect of relative humidity is only considered as a sink term of evapotranspiration but the modelling approach of evapotranspiration can be improved or relative humidity can be directly modelled; 3) One common problem about the CFD studies in urban microclimate is the assumption regarding the stability of the Atmospheric Boundary Layer (ABL). Especially during times with low wind speed, the assumption of neutral Atmospheric Boundary Layer might not yield correct results.

Considering the second part of the study where the effect of albedo on urban microclimate is investigated, the results are in line with the previous measurement studies, especially with the ones conducted by Doulos et al. [10]. In their study, Doulos et al. have investigated different pavement samples and for the samples which have an approximately 15% difference in albedo, they have measured a maximum surface temperature difference of 2.4°C and 2.1°C for concrete and stone materials, respectively. The difference in mean surface temperature was found to be 1.1°C for concrete and 1.5°C for stone. In this study, similar differences in surface temperatures were found.

7. Conclusions

Considering the global urbanization and the effect of urban microclimate on human thermal comfort and building energy demand, numerical studies regarding the analysis of urban climates will keep gaining popularity. CFD is one of the alternatives for the numerical analysis of urban microclimates, as demonstrated in previous studies.

In this paper, a two-part study is presented. In the first part, a series of unsteady CFD simulations considering wind flow and heat transfer are performed for the Bergpolder Zuid region in Rotterdam. The resulting surface temperatures are validated with the satellite imagery data for 15-19 July 2006. According to the results, CFD simulations have predicted the measured surface temperatures with an average deviation of 7.91%. In the second part of this study, the validated CFD approach is used to investigate the effect of surface albedo on the urban microclimate of Bergpolder Zuid region. The albedo values of the surfaces in the urban area are increased and decreased by 15% for the analysis. According to the results, it was found that increasing the albedo can decrease the average surface temperatures in the considered urban area by 2.18°C and decreasing the albedo can increase by 3.13°C. In addition, it was found that changing the albedo of the street material is more effective on average surface temperatures, compared with the changing the albedo of the building materials.

References

[1] United Nations. World Urbanization Prospects: The 2011 Revision. New York: 2012.
[2] Yow DM. Urban Heat Islands: Observations, Impacts, and Adaptation. Geogr Compass 2007;1:1227–51. doi:10.1111/j.1749-8198.2007.00063.x.
[3] Mirzaei PA, Haghighat F. Approaches to study Urban Heat Island – Abilities and limitations. Build Environ 2010;45:2192–201. doi:10.1016/j.buildenv.2010.04.001.
[4] Mills G. Urban climatology: History, status and prospects. Urban Clim 2014. doi:10.1016/j.uclim.2014.06.004.
[5] Blocken B. Computational Fluid Dynamics for urban physics: Importance, scales, possibilities, limitations and ten tips and tricks towards accurate and reliable simulations. Build Environ 2015;(article i. doi:10.1016/j.buildenv.2015.02.015.
[6] Erell E, Pearlmutter D, Williamson T. Urban Microclimate: Designing the Spaces Between Buildings. 1st ed. London: Earthscan; 2011.
[7] Toparlar Y, Blocken B, Vos P, Heijst G-J van, Janssen WD, van Hooff T, et al. CFD simulation and validation of urban microclimate: A case study for Bergpolder Zuid, Rotterdam. Build Environ 2015;83:79–90.
[8] Rosenfeld AH, Akbari H, Bretz S, Fishman BL, Kurn DM, Sailor D, et al. Mitigation of urban heat islands: materials, utility programs, updates. Energy Build 1995;22:255–65. doi:10.1016/0378-7788(95)00927-P.
[9] Chudnovsky a., Ben-Dor E, Saaroni H. Diurnal thermal behavior of selected urban objects using remote sensing measurements. Energy Build 2004;36:1063–74. doi:10.1016/j.enbuild.2004.01.052.
[10] Doulos L, Santamouris M, Livada I. Passive cooling of outdoor urban spaces. The role of materials. Sol Energy 2004;77:231–49. doi:10.1016/j.solener.2004.04.005.
[11] Prado RT a, Ferreira FL. Measurement of albedo and analysis of its influence the surface temperature of building roof materials. Energy Build 2005;37:295–300. doi:10.1016/j.enbuild.2004.03.009.
[12] Sailor DJ. Simulated Urban Climate Response to Modifications in Surface Albedo and Vegetative Cover. J Appl Meteorol 1995;34:1694–704. doi:10.1175/1520-0450-34.7.1694.
[13] Priyadarsini R, Hien WN, Wai David CK. Microclimatic modeling of the urban thermal environment of Singapore to mitigate urban heat island. Sol Energy 2008;82:727–45. doi:10.1016/j.solener.2008.02.008.
[14] Hamdi R, Schayes G. Sensitivity study of the urban heat island intensity to urban characteristics. Int J Climatol 2008;28:973–82. doi:10.1002/joc.
[15] Bretz S, Akbari H, Rosenfeld A. Practical issues for using solar-reflective materials to mitigate urban heat islands. Atmos Environ 1998;32:95–101. doi:10.1016/S1352-2310(97)00182-9.
[16] Klok L, Zwart S, Verhagen H, Mauri E. The surface heat island of Rotterdam and its relationship with urban surface characteristics. Resour Conserv Recycl 2012;64:23–9. doi:10.1016/j.resconrec.2012.01.009.
[17] Heusinkveld BG, Steeneveld GJ, van Hove LWA, Jacobs CMJ, Holtslag AAM. Spatial variability of the Rotterdam urban heat island as influenced by urban land use. J Geophys Res Atmos 2013. doi:10.1002/2012JD019399.
[18] Wieringa J. Updating the Davenport roughness classification. J Wind Eng Ind Aerodyn 1992;44:357–68.
[19] Van Hooff T, Blocken B. Coupled urban wind flow and indoor natural ventilation modelling on a high-resolution grid: A case study for the Amsterdam ArenA stadium. Environ Model Softw 2010;25:51–65. doi:10.1016/j.envsoft.2009.07.008.
[20] Franke J, Hellsten A, Schlünzen H, Carissimo B. Best practice guideline for the CFD simulation of flows in the urban environment. Hamburg: 2007.
[21] Tominaga Y, Mochida A, Yoshie R, Kataoka H, Nozu T, Yoshikawa M, et al. AIJ guidelines for practical applications of CFD to pedestrian wind environment around buildings. J Wind Eng Ind Aerodyn 2008;96:1749–61. doi:10.1016/j.jweia.2008.02.058.
[22] Richards P, Hoxey R. Appropriate boundary conditions for computational wind engineering models using the k-Ïµ turbulence model. J Wind Eng Ind Aerodyn 1993;46 & 47:145–53.
[23] Launder BE, Spalding DB. The numerical computation of turbulent flows. Comput Methods Appl Mech Eng 1974;3:269–89. doi:10.1016/0045-7825(74)90029-2.
[24] Cebeci T, Bradshaw P. Momentum Transfer in Boundary Layers. New York: Hemisphere Publishing Corporation; 1977.
[25] Blocken B, Stathopoulos T, Carmeliet J. CFD simulation of the atmospheric boundary layer: wall function problems. Atmos Environ 2007;41:238–52. doi:10.1016/j.atmosenv.2006.08.019.
[26] Shih T-H, Liou WW, Shabbir A, Yang Z, Zhu J. A new k-ϵ eddy viscosity model for high Reynolds number turbulent flows. Comput Fluids 1995;24:227–38.
[27] ANSYS Inc. ANSYS FLUENT 12.0 Theory Guide 2009.